Positioning sensory terminals in the olfactory lobe of *Drosophila* by Robo signaling

Dhanisha Jhaveri[1], Sumiti Saharan[1], Anindya Sen[1] and Veronica Rodrigues[1,2,*]

[1]Department of Biological Sciences, Tata Institute of Fundamental Research, Homi Bhabha Road, Mumbai 400005, India
[2]National Centre for Biological Sciences, TIFR, GKVK PO, Bangalore 560065, India
*Author for correspondence (e-mail: veronica@tifr.res.in)

Accepted 20 January 2003

Development 131, 1903-1912
Published by The Company of Biologists 2004
doi:10.1242/dev.01083

Summary

Olfactory receptor neurons and the interneurons of the olfactory lobe are organized in distinct units called glomeruli. We have used expression patterns and genetic analysis to demonstrate that a combinatorial code of Roundabout (Robo) receptors act to position sensory terminals within the olfactory lobe. Groups of sensory neurons possess distinct blends of Robo and Robo3 and disruption of levels by loss-of-function or ectopic expression results in aberrant targeting. In the wild type, most of the neurons send collateral branches to the contralateral lobe. Our data suggests that guidance of axons across brain hemispheres is mediated by Slit-dependent Robo2 signaling. The location of sensory arbors at distinct positions within the lobe allows short-range interactions with projection neurons leading to formation of the glomeruli.

Key words: Olfactory lobe, Sensory neurons, Robo receptors, Slit, Glomerular patterning

Introduction

The olfactory lobe of *Drosophila* shows a remarkable level of precision in its organization. Sensory neurons from the antenna project to the lobe and synapse with second-order interneurons within morphologically distinct structures called glomeruli (Stocker, 1994). The specificity of synapse formation is revealed by the targeting of neurons expressing individual odorant receptor genes to corresponding glomeruli within the lobe (Vosshall et al., 2000; Gao et al., 2000). Each glomerulus is identifiable by its size, shape and position, making developmental and functional analysis easier than in vertebrates (Laissue et al., 1999; Buck, 2000). The projection neurons, which are equivalents of vertebrate mitral/tufted cells, project from individual glomeruli to higher centers in the calyx of the mushroom bodies and lateral horn (Stocker et al., 1990; Jefferis et al., 2001; Jefferis et al., 2002; Marin et al., 2002; Wong et al., 2002). These neurons, together with local interneurons that connect between glomeruli, provide circuitry for information processing, involving integration of sensory input with possible feedback from more central pathways (Fiala et al., 2000; Ng et al., 2002; Wang et al., 2003). An understanding of how this highly stereotyped network arises during development will help elucidate general rules governing circuit design in phylogenetically distinct organisms.

The development of pattern within brain structures can be addressed at two levels. First, what are the mechanisms by which individual sensory neurons and their target interneurons find each other? Second, how are these synapses located reproducibly within the three-dimensional architecture of the neuropil? Studies in the *Drosophila* embryo have provided valuable insights about how axonal scaffolds and synapses are organized within the axis of the embryonic midline (Dickson, 2001; Grunvald and Klein, 2002; Ziatic et al., 2003). This instruction involves a combinatorial expression of receptors on the axonal surface, and attractive and repulsive ligands secreted at the midline. It is becoming increasingly clear that similar principles could apply in patterning more complex three-dimensional contours in adult brains (Richards, 2002; Bagri et al., 2002; Hutson and Chien, 2002; Plump et al., 2002).

In the olfactory system of both vertebrates and insects, neurons expressing a given odorant receptor gene project with remarkable precision to specific glomerular sites within the olfactory lobe. In rodents, the specificity of axonal convergence is mediated by the odorant receptors (Wang et al., 1998) in collaboration with cell-surface molecules – the Ephrin A proteins (Cutforth et al., 2003). In *Drosophila*, the SH2/SH3 adaptor, Dreadlocks (Dock) and serine/threonine kinase Pak, form part of a signaling module that is necessary for the precise guidance of olfactory neurons to their glomerular targets (Ang et al., 2003). Dock and Pak are known to be downstream of receptors that play key roles in axon guidance, such as the Down Syndrome Cell Adhesion Molecule (Dscam) (Schmucker et al., 2000) and the Roundabout (Robo) family (Fan et al., 2003)

Loss of *Dscam* function affects the development of olfactory projections; neurons enter the lobe but terminate inappropriately at ectopic sites (Hummel et al., 2003). As *Dscam* can theoretically encode 38,000 isoforms by alternative splicing, this locus provides an intriguing means by which axons can recognize their postsynaptic partners. Interestingly, 68 combinations of transcripts have been detected in olfactory neurons. The dendritic arborization of projection neurons within specific glomeruli has been shown to occur prior to the arrival of the sensory neurons into the lobe (Jefferis et al.,

2003). The mechanism of projection neuron patterning is therefore likely to be independent of sensory neurons and has been shown to require the POU domain transcription factors Drifter and Acj6 (Komiyama et al., 2003). How are sensory neuron arbors correctly positioned to allow interaction with appropriate neural partners?

In this paper, we investigate the role played by Robo receptors as possible guidance cues during formation of the olfactory map. A precedent for the role of Robo/Slit mediated signaling in determining topographic projections exists in the vomeronasal system of the rodent (Knoll et al., 2003). We demonstrate that a combinatorial code, defined by the domains and levels of Robo receptors, patterns not only the location of glomeruli but also the formation of the commissures which connect the two lobes. Our results from loss-of-function and gain-of-function analysis suggest that Robo receptors together with their ligand Slit are involved in positioning the arbors of the olfactory neurons at defined sites within the lobe.

Materials and methods

Fly stocks

SG18.1-Gal4 (Shymala and Chopra, 1999), *lz-Gal4* (Lebetsky et al., 2000), *ato-Gal4* (Hassan et al., 2000), *Or22a-Gal4* and *Or47b-Gal4* (Vosshall et al., 2000) strains were used to analyze olfactory neurons. For ectopic expression of Robo receptors, we used *UAS-robo*(2X), *UAS-robo3* and EP2582 (*UAS-robo2*) obtained from the Dickson laboratory (Rajgopalan et al., 2000a; Rajgopalan et al., 2000b); and *UAS-robo* from the Goodman laboratory (Simpson et al., 2000a; Simpson et al., 2000b). *UAS-comm* and *UAS-slit* were kindly provided by Guy Tear (Kidd et al., 1999); *UAS-N-sybGFP* (UNG12) by Mani Ramaswami; *loco-Gal4*, *slit-Gal4* and *slit-lacZ* by Gerd Technau; *GH146-Gal4* by Reinhard Stocker; and *ato*^{1}/TM3, Df(3R)*p*^{13}/TM3 and *UAS-ato* by Andrew Jarman. Mutant alleles *y,w*; *robo2*^{1}/ *CyO wglacZ* and *y,w*; *robo3*^{1}/ *CyO wg lacZ* were obtained from B. Dickson. The deficiency uncovering the *slit* locus Df(2R)WMG, *wg*$^{Sp-1}$ *Bl*^{1} *lt*^{1} /In(2LR)*Gla, wg*$^{Gla-1}$(52A9-10;52D9-15); the FRT stocks *yw*; P{ry+t7.2=neoFRT}40A/*CyO*; *Tub-Gal80 FRT40A*; *ey*-FLP; *UAS Cdc42*.^{V12} and balancer stocks were obtained from the *Drosophila* Stock Center at Bloomington, Indiana. EP31010 (*UAS-abl*) was obtained from the *Drosophila* Stock Center at Szeged.

All fly stocks were grown on standard cornmeal medium at 25°C. White prepupae (0 hours after puparium formation; APF) were collected and allowed to develop on moist filter paper. This stage lasts 1 hour, hence the error in staging is ±30 minutes. Wild-type pupae take about 100 hours to eclose when grown at 25°C in our laboratory.

Clonal analysis

Clones of *robo* mutants were generated using the mosaic analysis with repressible cell marker (MARCM) method described by Lee and Luo (Lee and Luo, 1999). Stocks of FRT40A *robo2*^{1}/*CyO* FRT40A and *robo3*^{1}/*CyO* were generated using standard recombination. Males of genotype *Or-22a-Gal4;robo2*^{1} (or *robo3*^{1}) FRT40A/*CyO;ey-Flp*/+ were crossed to *Tub-Gal80* FRT40A/*CyO*;UNG12/*TM6-Tb* females. Non-*CyO*, non-*Tb* flies were dissected and stained with antibodies against GFP and mAbnc82 (see below). GFP expressing neurons are homozygous for the mutation. To ascertain the efficiency of *eye*-Flp, we crossed *eye*-Flp/TM6-*Tb* flies with *Act5C*>CD2>Gal4, *UAS-nlsGFP*. All non-*Tb* flies showed GFP expression in the entire eye antennal disc. The brains of these animals did not show any clones in the cells around the olfactory lobes, establishing that *eye*-Flp generates clones only in the sensory neurons of the olfactory system.

Immunohistochemistry

Dissection and antibody staining of pupal and adult brain whole mounts were carried out as described previously (Jhaveri et al., 2000). Where mAbnc82 was to be used, the protocol of Laissue et al. (Laissue et al., 1999) was followed. The primary antibodies used were anti-Robo (1:10 from Corey Goodman), anti-Robo2 (1:200 from Corey Goodman), anti-Robo3 (1:100 Developmental Studies Hybridoma Bank at University of Iowa), mouse anti-Slit (1:50 from Spryos Artavonis-Tsakonis), mAbnc82 (1:10 from E. Buchner), rabbit anti-GFP (1:10,000 from Molecular Probes) and rabbit anti-Repo (1:5,000 from S. Susinder). Secondary antibodies used were Alexa 488- and Alexa 568-coupled goat anti-mouse and anti-rabbit IgG (1:200 Molecular Probes). Labeled samples were mounted in anti-fading agent, Vectashield (Vector Laboratories) imaged on BioRad Radiance 2000 at 1 μm intervals; data were processed using Confocal Assistant 4.2 and Adobe Photoshop 5.5.

In order to quantitate staining intensity, the regions of interest on 0.7 or 1 μm sections were demarcated and pixel intensity was estimated using Image J software. The cumulative intensity over the volume of the glomerulus (for Robo experiments) or the entire lobe (for Slit experiments) was estimated.

Results

Potential role for a code in olfactory neurons is suggested by Robo localization

The *Drosophila* olfactory lobe comprises about 50 glomeruli located at fixed positions within the mediolateral, anteroposterior and dorsoventral axis (Fig. 1A). Sensory neurons expressing a given candidate odorant receptor (Or) target to the same glomeruli (Fig. 1B) and also send projections to the contralateral lobe (Fig. 1A,B, arrow). Previous work (Jhaveri et al., 2000) has shown that adult olfactory neurons differentiate within the first one-third of pupal life, radiate over the lobe anlage and transit across the midline (Fig. 1C). Sensory neurons invade the lobe during the next one-third of pupation and form distinct glomeruli (Fig. 1D).

We have used antibodies against the three Robo receptors to examine their localization in olfactory neurons during pupal life. The patterns of Robo, Robo2 (Lea – FlyBase) and Robo3 are rather dynamic and appear markedly different when examined early during lobe development (Fig. 2A-D), when compared with later after glomeruli are formed (Fig. 2G-I). During the first ~20 hours after puparium formation (APF), when the olfactory neurons are on the surface but have not yet invaded the lobe, Robo is expressed uniformly on all afferent axons (arrowhead in Fig. 2A,D). Robo2 is present at low levels in all neurons but is enriched in regions lateral to the commissure (red arrows in Fig. 2B). A careful examination of confocal sections through a number of pupal lobes stained with anti-Robo2 suggests that immunoreactivity is lower as axons transit the midline (white arrow in Fig. 2B,D) than just prior to/after crossover. Expression of Robo2 declines in older pupae and is no longer detectable by ~40 hours APF (not shown). Axons that express high Robo3, lie at more medial positions in the outer nerve layer (red arrows in Fig. 2C,D). The analysis of patterns of expression indicates that populations of neurons possess unique combinations of Robo, Robo2 and Robo3 that change during development.

Ziatic et al. (Ziatic et al., 2003) showed that *robo3* expression in the embryonic peripheral nervous system is regulated by the proneural gene *atonal* (*ato*). In the adult olfactory system, *ato* specifies a subset of neurons that are the first to develop and appear to guide the rest of the axons into the lobe (Jhaveri and Rodrigues, 2002). In *ato*^{1}/Df(3R)p^{13}

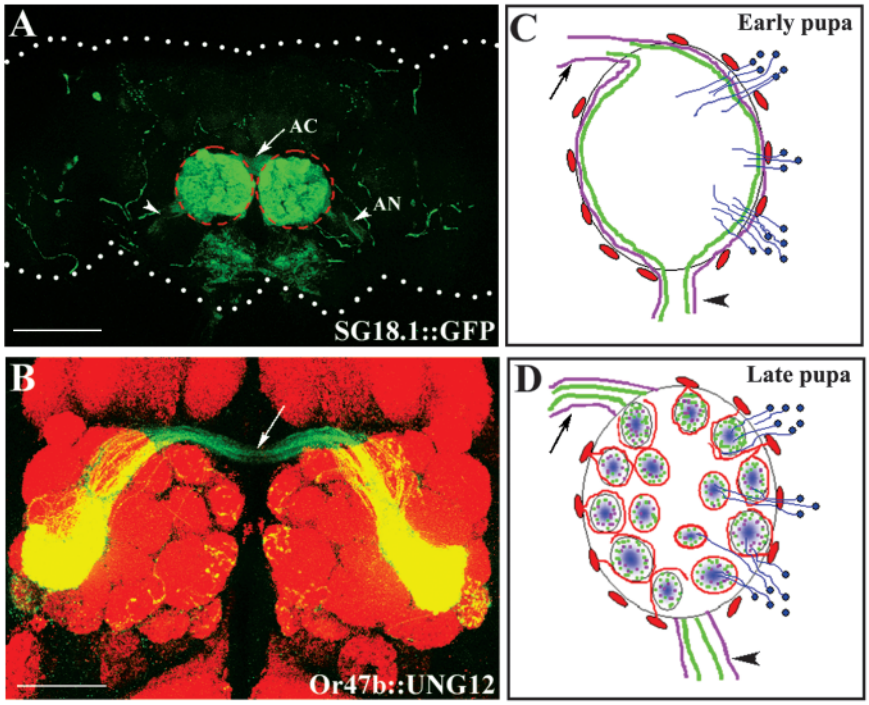

Fig. 1. Development of the olfactory lobe in *Drosophila*. (A) Olfactory lobes (encircled with broken red lines) are visualized in the brain (marked with broken white lines) by expression of GFP driven by *SG18.1-Gal4*. Neurons enter the lobe through the antennal nerve (AN) and cross over to the contralateral side through the antennal commissure (AC). Scale bar: 100 μm. (B) Olfactory lobes of *Or47b-Gal4/+;UAS-NsybGFP* (UNG12)/+ stained with mAbnc82 (red). Projections to the glomerulus VA1 can be seen (arrow indicates the AC). Scale bar: 50 μm. (C,D). Schematic diagrams summarizing cellular events occurring during lobe development in the early (C) and late pupa (D). In the early pupa (~18-30 hours APF), sensory neurons enter the brain via the antennal nerve (arrowhead) and traverse in the outer nerve layer in close association with glial cells (red). Ato-derived 'pioneer' neurons arrive at the lobe first (purple) and guide the rest of the neurons (green) to the antennal commissure (arrow). At this time, the projection neurons (blue) are already present within the lobe. Sensory neurons invade the lobe from about 25 hours APF. (D) Termination of sensory neurons (green) and their contact with appropriate projection neurons (blue) is followed by ensheathing of the neural elements to form glomeruli.

animals, these 'pioneers' fail to form and the rest of the neurons stall at the entry to the olfactory lobe. A subset of the Ato-independent neurons express Robo3 (arrows in Fig. 2E). Furthermore, only a subset of the Ato-dependent neurons visualized by Ato::GFP express Robo3 (Fig. 2F). As expected, these occupy medial positions in the outer nerve layer (arrows in Fig. 2F). These data together suggest that Robo3 is not expressed in genetically defined subset of neurons in the pupal olfactory system.

Sensory neurons begin to invade the lobe from about 25 hours APF and the first signs of glomerular organization become apparent by around 36 hours APF (Jhaveri et al., 2000; Jefferis et al., 2003). Glomerular formation occurs sequentially and by 60 hours APF most of the glomeruli have formed. The entry of glial cell processes and concomitant increase in lobe volume, results in some re-organization of glomerular position and the adult pattern (Fig. 2J) can only be discerned by about 80 hours APF. Robo and Robo3 are enriched in subsets of sensory neurons as they terminate within the lobe (Fig. 2G-I). Robo is detected in most axons, although at differing levels (Fig. 2G,I), while Robo3 is strongly enriched in terminals within a smaller number of glomeruli (Fig. 2H,I). A comparison of stained 60 hour APF lobes (Fig. 2H,I) with the adult glomerular map (Fig. 2J) suggests that Robo3-expressing neurons tend to preferentially target more dorsomedial locations. An estimation of Robo and Robo3 immunoreactivity in identified glomeruli supports the idea of a combinatorial code in determining sensory neuron position (Table 1).

We stained brains of different pupal ages with antibodies against the secreted ligand Slit (Rothberg et al., 1990; Kidd et al., 1999). A sheet of cells in the midline of the sub-esophageal ganglion expresses high levels of Slit (arrowheads in Fig. 2K).

Table 1. Distribution of Robo3 and Robo receptors among olfactory glomeruli

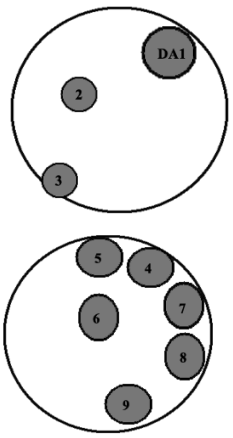

Glomerulus	Average intensity/pixel	
	Robo3	Robo
DA1	106.6	143.5
2	134.0	–
3	122.5	76.1
4	117.5	135.7
5	92.8	–
6	84.4	–
7	74.2	152.8
8	27.4	146.0
9	–	112.3

A set of Robo3-positive 'glomeruli' were selected in 60 hour APF olfactory lobes and examined for Robo. The altered morphologies of pupal 'glomeruli' prompted us to adopt an arbitrary nomenclature rather than that of Laissue et al. (Laissue et al., 1999). DA1 is recognisable. The intensities of Robo3 and Robo in eight glomeruli were estimated as described in methods. Glomerulus '9' is an example of a glomerulus with Robo but no Robo3 expression.

Immunoreactivity declines in later pupae (after 60 hours APF) and is absent in the adult. The midline cells do not express the glial marker Reverse Polarity (Repo) (red in Fig. 2K). Other

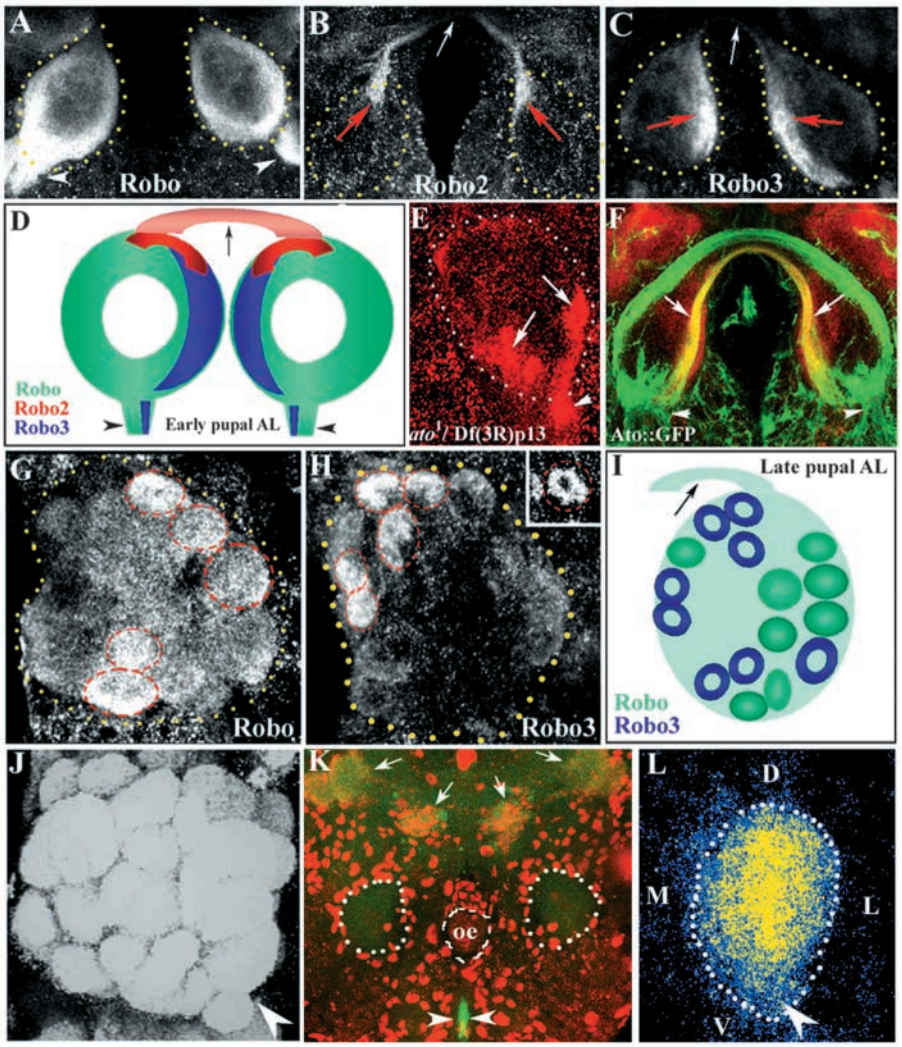

Fig. 2. Localization of Robo receptors during olfactory lobe development. Lobes are outlined by broken lines and oriented with antennal nerve at the bottom of each picture (arrowheads in A,D,E,F,J,L). Confocal imaging was from anterior to posterior and a few 1 μm confocal sections at the relevant level are stacked in each picture. The lateral (L), medial (M), ventral (V) and dorsal (D) coordinates are as indicated in L. (A-D) Twenty-four hours APF. Robo (A) is localized uniformly in the axons within the antennal nerve (arrowheads). Robo2 (B) is enriched lateral to the commissure (red arrows) and is reduced within the midline (arrow). Robo3 (C) is localized in axons that lie medially within the outer nerve layer (red arrows). Expression is also detected at the midline (arrow). (D) Diagram summarizing expression pattern in the early pupal stages (~18 to 30 hours APF). Arrowhead indicates antennal nerve; arrow indicates antennal commissure. (E) Pupal olfactory lobe from *ato*^{1}/Df(3R)*p*^{13} stained with anti-Robo3. In the absence of Ato-dependent neurons, the rest of the axons stall after their entry in the antennal nerve (arrowhead). Robo3 is expressed in several terminals (arrows). (F) Thirty-hour APF *ato-Gal4/UAS-GFP* pupa stained with anti-Robo3 (red). The Ato-dependent neurons (green) can be seen in the outer nerve layer around the olfactory lobes and cross over in the antennal commissure. Robo3-expressing axons are located medially in the outer nerve layer (arrows). (G-I). Robo and Robo3 expression at 60 hours APF. Glomeruli that express high Robo (G; indicated by broken red lines) can be distinguished from the lower level expression. Robo3 is localized at high levels (H; indicated by broken red lines) in a small subset of glomeruli (depicted in blue in I). Immunoreactivity is enriched at the sensory terminals, which lie on the periphery of the glomerulus (inset in H). (I) Diagram representing Robo (green) and Robo3 (blue) localization among 'glomeruli'. Entire confocal stacks from several stained lobes were examined. The pictures in G,H are from only a few sections through the lobe and not all stained glomeruli have been shown. (J) *z*-stack of an olfactory lobe stained with mAbnc82 showing the positions of glomeruli in the adult. Gaps between glomeruli are normally occupied by glial processes. (K) Twenty-hour APF brain stained with anti-Slit (green) and anti-Repo (red). A row of cells at the midline (arrowheads) of the ventral sub-esophageal ganglion (oe, esophagus) as well as regions in the mid-brain (arrows) are recognized by anti-Slit. Olfactory lobes (outlined by broken lines) are demarcated by glial cells and the Slit immunoreactivity in this neuropil was estimated using the Image J software (L). Pixel intensities were estimated in 1 μm sections through the lobe and summed. Low and high intensity levels are pseudo-colored blue and yellow, respectively.

regions in the midbrain closely associated with groups of Repo-positive glial cells were also labeled by anti-Slit (arrows in Fig. 2K). The diffuse nature of the staining makes it difficult to ascertain whether the glia are the source of secreted Slit in the midbrain. At 20 hours APF, the boundaries of the olfactory lobes are clearly demarcated by the presence of surrounding glial cells (broken lines in Fig. 2K). Slit levels within the lobe neuropil is significantly higher than that of the background (Fig. 2L). Expression can be detected from 14 hour APF and begins to decline by 60 hours APF (not shown).

Loss of Robo function reveal a function in olfactory neuron targeting and lobe organization

The MARCM method (Lee and Luo, 1999) combined with ey-FLP (Newsome et al., 2000) generates large patches of homozygous tissue in the eye-antennal disc (Ang et al., 2003; Jefferis et al., 2003). As flip-out occurs early, phenotypes generated in mature neurons result from a lack of gene function from the beginning of differentiation. We generated clones of *robo2*^{1} and *robo3*^{1} and examined targeting of a small number of sensory neurons marked by the *Or22a-Gal4* transgene. Sensory neurons expressing Or22a normally project to glomerulus designated DM2 (Fig. 3A) (Vosshall et al., 2000) and cross-over to the contralateral lobe in the inter-antennal commissure (arrow in Fig. 3A).

Neurons lacking Robo2 function (*robo2*^{1} clones) fail to cross over to the contralateral lobe and terminate at the midline forming small 'glomerular-like' structures (arrowheads in Fig.

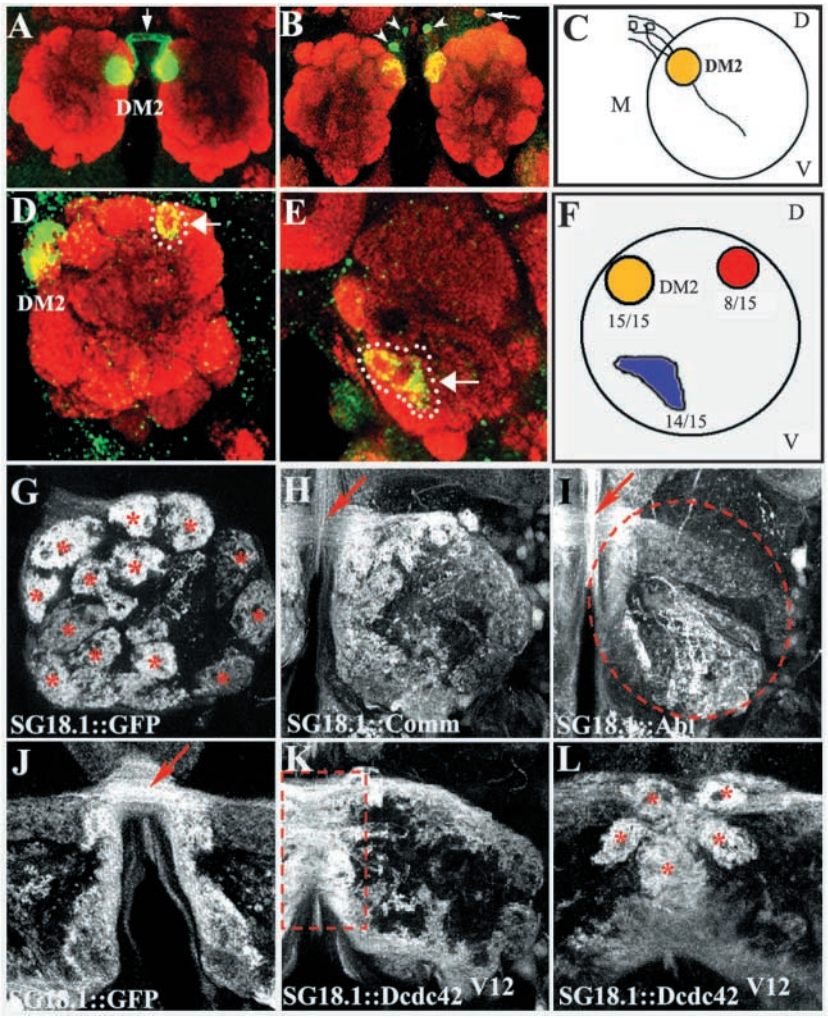

Fig. 3. Robo receptors regulate targeting of olfactory neurons to specific glomeruli. Lobes are oriented as indicated in C,F: M, medial; D, dorsal; V, ventral. Imaging was carried out from anterior to posterior and a few 1 μm confocal sections are stacked in each picture. (A) Olfactory lobes of *or22a-Gal4;UAS-N-SybGFP* stained with mAbnc82 (red). Or22a-expressing neurons project to a single glomerulus DM2 and also cross over in the inter-antennal commissure (arrow). (B,D,E) The MARCM method was used to positively mark neurons mutant for *robo2*^{1} (B) or *robo3*^{1} (D,E). Axons lacking Robo2 function terminate within the midline creating a 'roundabout' appearance (arrowheads in B; diagram in C). Ectopic axonal arbors are immunoreactive for mAbnc82 (arrow in B). Axons lacking Robo3 function terminate aberrantly (broken lines in D,E; diagram in F). (G-L) Sensory neuron terminals in the olfactory glomeruli are visualized using a *SG18.1-UAS-GFP* recombinant strain in different conditions. (G,J) Appropriate confocal sections have been selected to visualize normal glomeruli (G, *) and antennal commissure (J, arrow). (H) *SG18.1 UAS-GFP/UAS-comm*. (I) *SG18.1 UAS-GFP/UAS-abl.* In both H and I, glomerular patterning is significantly disrupted while the antennal commissure is present (arrow), although axons appear somewhat loosely fasciculated. (K,L) *SG18.1 UAS-GFP/UAS-Dcdc42*^{v12} (constitutively active). Glomeruli cannot be discerned within the lobes (K). The commissural region (boxed in K) is examined at better resolution in L. Stacking of fewer sections shows a clear glomerular-like organization (*) within the commissure.

3B,C). The terminals showed immunoreactivity against the synaptic marker nc82 (arrow in Fig. 3B). Targeting to DM2 occurred normally although in many (13 out of 16) cases the glomeruli appeared less intensely innervated by GFP-expressing neurons. Loss of Robo3 function (*robo3*^{1} clones), however, affected targeting of axons rather dramatically (Fig. 3D-F). In all cases, some mutant neurons did project correctly to DM2 (Fig. 3D,F) although a subset of axons strayed to ectopic sites (arrows in Fig. 3D,E). Commissure formation was unaffected (not shown). The erroneously placed terminals formed 'glomerular-like' organizations as revealed by staining with mAbnc82, but these did not correspond in shape or position to those previously identified by Laissue et al. (Laissue et al., 1999). A large irregular shaped 'glomerulus' located ventrally in the posterior region of the lobe was most frequently observed (Fig. 3E,F). In about half the preparations, an additional site was observed in a dorsolateral location (Fig. 3D,F). We ascertained that such ectopic targets were never found in control animals carrying the *or22a-Gal4* (14.6) transgene (Bhalerao et al., 2003).

As Robo is expressed rather generally in olfactory neurons, we decided to study loss-of-function by targeted misexpression of antagonists of signaling (Dickson, 2001), rather than in clones. *SG18.1-Gal4* expresses in a large fraction of olfactory neurons thus revealing most of the glomeruli (Fig. 3G, asterisks) as well as the antennal commissure (arrow in Fig. 3J). Ectopic expression of *commissureless* (*comm*) (Kidd et al., 1998) using *SG18.1-Gal4* resulted in disorganization of glomerular patterning (compare Fig. 3H with 3G) with a weak effect on the commissure (arrow in Fig. 3H). Comm has been shown to downregulate Robo, although its effect on Robo2 and Robo3 is less well understood (Rajagopalan et al., 2000a; Rajagopalan et al., 2000b). The phenotype of Comm ectopic expression suggests that Robo is necessary for determining sensory neuron position within the lobe. Abelson kinase (Abl) phosphorylates the CC0 and CC1 domains of Robo, thus antagonizing signaling (Bashaw et al., 2000). Ectopic expression of either Abl or a constitutively active Dcdc42^{v12} completely abolishes glomerular formation (Fig. 3I,K). Sensory neurons expressing Dcdc42^{v12} (SG18.1::Dcdc42^{v12}) show an attraction for the midline and terminate there forming 'glomerular-like' structures at the midline (Fig. 3L, asterisks). Results from loss-of-function clones predict such a phenotype for *robo2* nulls. Constitutive activation of Dcdc42 is known to affect cytosketal dynamics generally, and could phenocopy a loss-of-function of all Robo receptors (Fritz and VanBerkum, 2002).

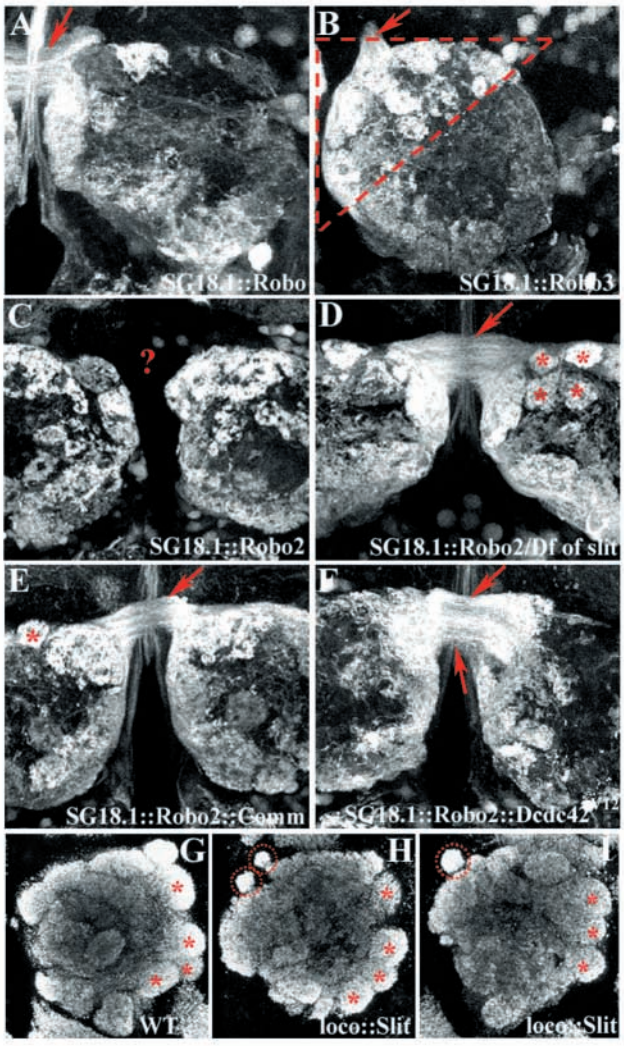

Fig. 4. Robo/Slit-dependent signaling regulates glomerular patterning. Orientation is as described for previous figures. (A-F).The *SG18.1-Gal4 UAS-GFP* recombinant line was used to visualize sensory neuron within the lobe and also to misexpress genes under UAS control. (A) *SG18.1-Gal4 UAS-GFP/UAS-robo;UAS-robo(2X)/+* (three copies). Glomerular formation is abrogated but the commissure is still present (arrow). (B) *SG18.1-Gal4 UAS-GFP/UAS-robo3*. Positions of most terminals are shifted to the dorsomedial location within the lobe (indicated with broken red lines). Commissure is unaffected (arrow) (C) *SG18.1-Gal4 UAS-GFP/UAS-robo2*. ? indicates the position of the commissure that is absent. (D) *SG18.1 UAS-GFP UAS-robo2/Df(2R) WMG* (*Df(2R)Slit*). Commissure (arrow) formation is restored when dose of the Slit ligand is reduced by half. Glomerular morphology is also restored (asterisks). (E) *SG18.1 UAS-GFP UAS-robo2/UAS-comm*: partial restoration of glomerular morphology (*) and complete rescue of the commissure (arrow). (F) *SG18.1 UAS-GFP UAS-robo2/UAS-Dcdc^{v12}*. The commissure is present but sensory axons are much more loosely packed than in the normal (arrows). (G-I) Adult olfactory lobes stained with the synaptic marker mAbnc82. (G) Normal controls. (H,I) *loco-Gal4/UAS-Slit:* ectopic glomeruli are circled by broken red lines. Only a few glomeruli are recognizable when Slit is ectopically expressed (marked by an asterisk).

Ectopic expression demonstrates that levels and location of Robo receptor expression are important for three-dimensional patterning of sensory terminals

We ectopically expressed Robo in sensory neurons to test whether the domains and levels of receptors are instructive in positioning of sensory terminals within the lobe. *SG18.1::GFP* was used to drive Robo in olfactory neurons; the positions and morphology of glomeruli could be visualized by GFP. Robo is expressed endogenously in all olfactory neurons and the small increase in level caused by driving a single copy of the *UAS-robo* transgene did not significantly alter lobe morphology (not shown). Higher levels achieved by driving three copies of the transgene abrogated glomerular formation (Fig. 4A). Changing the nature of the Robo code by misexpressing Robo3, however, resulted in a dorsomedial shift of projections (Fig. 4B). The commissure forms normally when either Robo or Robo3 are misexpressed (red arrows in Fig. 4A,B). Ectopic expression of Robo2, however, completely abolishes commissure formation with a less severe effect on glomerular morphology (Fig. 4C).

Next, we tested whether the genetic elements participating with Robo signaling in other well-studied systems also operated in the *Drosophila* adult olfactory system (Grunwald and Klein, 2002). We crossed a deficiency for the Slit region into an *SG18.1 UAS-GFP UAS-robo2* recombinant. In this situation, where endogenous levels of the ligand were reduced by 50%, commissure formation, which is disrupted by the ectopic expression of Robo2, was restored and glomerular morphology also returned to normal (Fig. 4D). Targeted down-regulation of Robo signaling by misexpression of Comm (Fig. 4E) or activated Dcdc42^{v12} (Fig. 4F), respectively, also suppress the phenotype caused by elevated Robo2.

Results presented above argue that sensory neuron positioning within the lobe is determined by signaling through the Robo receptors. Reduction of Slit levels suppress the effect of receptor overexpression, demonstrating that the phenotypes are mediated through endogenous ligand. In this case, alteration of the geometry of the Slit gradient by misexpression would be expected to alter terminal positioning of sensory neurons. We drove high Slit expression in glial cells around and within the lobe using *loco-Gal4* (data not shown) (Jhaveri et al., 2000). Staining of the adult lobes in these animals with an antibody against the synaptic marker mAbnc82 revealed the presence of ectopic glomeruli outside the normal lobe circumference (broken lines in Fig. 4H,I). Increasing Slit levels further using multiple copies of the transgene led to more severe effects.

Will perturbation of Robo levels in specific neurons result in changes in their three-dimensional organization?

Our model proposes that olfactory neurons traveling in the outer nerve layer possess a different combination of Robo receptors that respond to Slit by branching into the lobe and arborizing at specific positions. In order to understand this positional code, we selected a Gal4 line that would allow us to drive expression in a set of neurons projecting to identified glomeruli from early during development. *lz-Gal4*;*UAS-GFP* labels two glomeruli – DM6 and DL3 – during development and in the adult brain (Fig. 5A-D), thus providing a means to examine the location of selective sensory neurons when the combinations of Robo are altered. We found that a change in

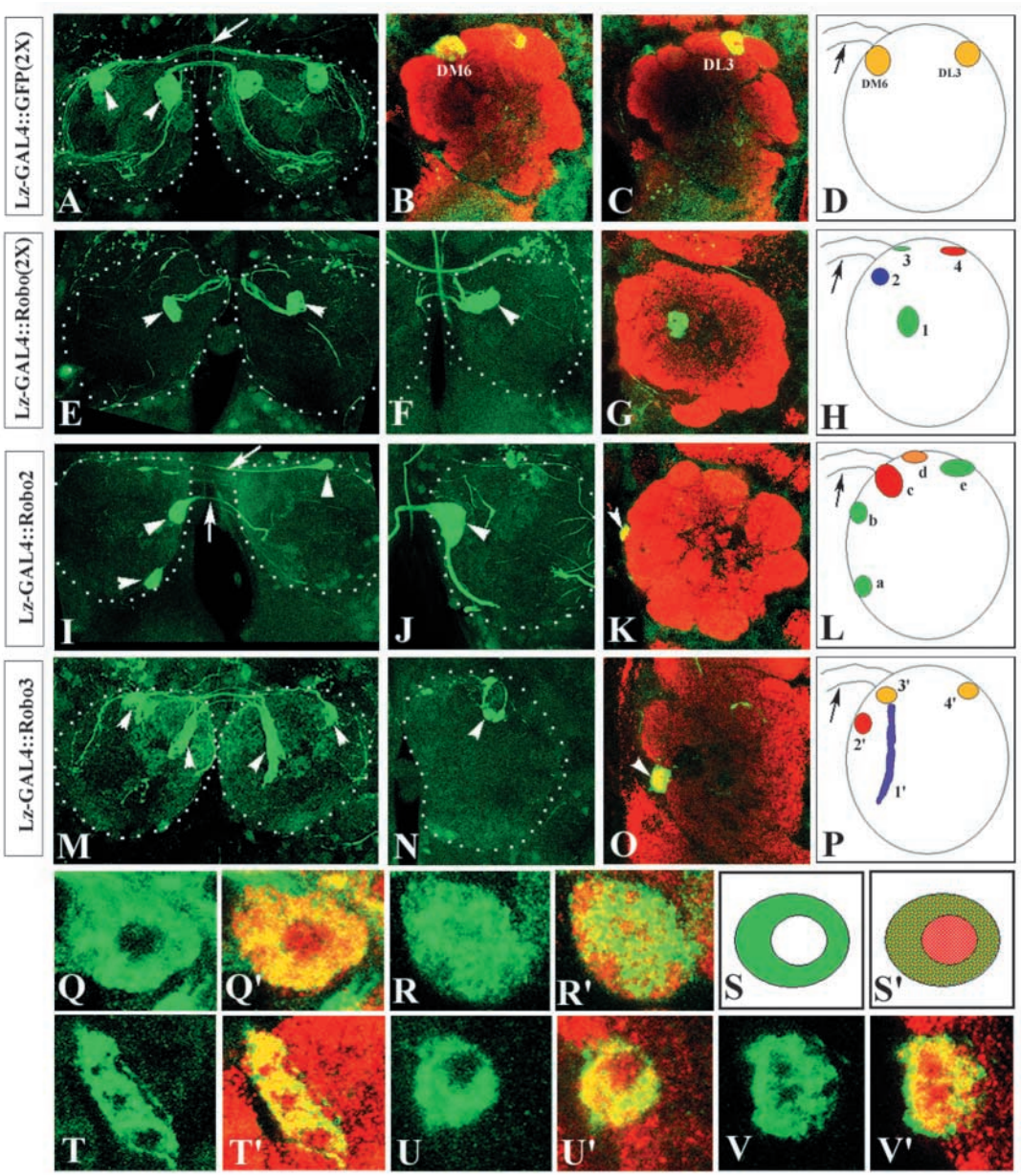

Fig. 5. Robo misexpression shifts location of sensory arbors in the olfactory lobe. (A-P) Orientation of the olfactory lobes is as described in the previous figures. Relevant 1 μm confocal sections are stacked in each picture (green). B,C,G,O are also labeled with the synaptic marker mAbnc82 (red). The diagrams in D,H,L,P depict the positions of sensory terminals depicted from several preparations. Colors indicate the anterior to posterior location of the terminals as observed in confocal imaging of the lobe. Violet is most anterior, followed by blue, green, yellow, orange with red appearing most posteriorly. Arrows indicate the antennal commissure. Quantitative results are presented in Table 2. (A-D) *lz-Gal4/+;UAS-GFP/+*. Axons project to two glomeruli (arrowheads in A) and cross over in the antennal commissure (arrow in A). Staining with mAbnc82 (B,C) allowed identification of these glomeruli as DM6 and DL3 (diagram in D). (E-H) *lz-Gal4/+;UAS-GFP/UAS-robo*. Sensory terminals located centrally within the lobe (arrowheads). (I-L) *lz-Gal4/+;UAS-GFP;UAS-robo2*. Targets to only one lobe were frequently observed (arrowheads in I). (M-P) *lz-Gal4/+;UAS-GFP/UAS-robo3.* Sensory neurons terminate at ectopic positions and often show altered morphologies (arrowheads). (Q-V) Cytoarchitecture of individual glomeruli. (Q,S) Visualization of *SG18.1-Gal4;UAS-GFP* show that sensory arbors (green) are located in a 'doughnut-like' arrangement on the periphery of the glomerulus. (Q′,S′) staining with the synaptic marker mAbnc82 (red) shows presence of synapses within the outer region (yellow) as well as the core of the glomerulus. (R,R′). *GH146 UAS-GFP* (green) shows position of projection neurons within the glomerulus. These neurons arborize within the entire glomerulus as can be seen with the overlap with mAbnc82 staining (red, R′). (T-V) Three examples of ectopic glomeruli generated by misexpression of Robo receptors show comparable organization of sensory neurons and interneurons. The sensory neurons are located on the peripheries (T,U,V) and the staining with mAbnc82 highlights both peripheral and central regions of the glomerulus (T′,U′,V′).

the levels of any of the three Robo receptors, caused by misexpression using the *lz-Gal4* driver, altered the positions of these identified terminals (Fig. 5E-P). The phenotypes showed variable expressivity; however, we were able to categorize preferred positions for the terminals in each treatment (Fig. 5D,H,L,P; Table 2).

Table 2. Location of sensory terminals after ectopic expression of Robo receptors in sensory neurons

	DM6	DL3			
lz-Gal4::GFP	8/8	8/8			
	Position 1	**Position 2**	**Position 3**	**Position 4**	
lz-Gal4::Robo	16/28	5/28	2/28	1/28	
	Position a	**Position b**	**Position c**	**Position d**	**Position e**
lz-Gal4::Robo2	2/32	8/32	10/32	3/32	2/32
	Position 1′	**Position 2′**	**Position 3′**	**Position 4′**	
lz-Gal4::Robo3	8/42	21/42	8/42	16/42	

In *lz-Gal4;UAS-GFP*, sensory projections to DM6 and DL3 are visualized. An arbitrary nomenclature is adopted to describe positions adopted by neurons ectopically expressing Robo (1-4), Robo2 (a-e) and Robo3 (1′-4′). Refer to Fig. 5 for details.

Elevated Robo levels shift DL3/DM6 neurons to more central locations (arrowheads in Fig. 5E,G; 1 in H). Robo3 misexpression shifted the positions of the arbors most frequently to a mediodorsal axis (Fig. 5M-P). Large irregular-shaped glomeruli (arrowhead in Fig. 5M, 1′ in P) were frequently observed (Table 2). The changes in neuronal positions observed by Robo2 misexpression (Fig. 5I-L) were somewhat surprising given our hypothesis that Robo2 is involved largely in commissure formation. We suggest that high levels of Robo2 induced by *lz-Gal4* could interfere with the function of endogenous receptors. Robo2 misexpression most frequently produced cases where projections were seen terminating within a single lobe (arrowheads in Fig. 5I).

The ectopic ‘glomeruli’ produced by alterations in the Robo code showed a normal organization of cellular elements (Fig. 5Q-V). In the wild type, terminal branches of sensory neurons remain at the periphery of each glomerulus (Fig. 5Q,S). Dendritic arbors of the lobe interneurons, filled the entire glomerulus as seen by GFP driven by *GH146-Gal4* (Jefferis et al., 2001) (Fig. 5R, green) or the synapse specific marker mAbnc82 (Fig. 5Q′,R′,S red). Glomeruli produced by misexpression of any of the Robo receptors also showed a similar organization as evidenced by mAbnc82 staining (Fig. 5T-V).

Our expression and genetic data allows us to propose the model summarized in Fig. 6. Neurons arriving at the olfactory lobe in the antennal nerve express Robo, and those expressing high levels of Robo3 additionally decussate onto the medial side of the outer nerve layer (Fig. 6A). The position of an axon in the nerve layer is influenced by Slit levels, although the identity of the cells that contribute Slit still needs to be elucidated. Several regions of Slit expression have been detected in the brain, although the cells at the midline express highest levels. Robo2, which is expressed at very low levels in all sensory neurons, is elevated after they cross the midline thereby preventing re-crossing. Later during pupation (Fig. 6B), sensory axons branch into the lobe and terminate at distinctive positions regulated by their unique Robo code in response to Slit levels. This allows short-range interactions with the dendritic arbors of projection neurons leading to formation of glomeruli.

Discussion

Conserved mechanisms for pathway choice

Our results, taken together with findings from a wide variety of tissues and organisms, suggest the following steps by which precise patterning of brain regions take place during development. Regional specification of ectodermal tissues selects neuronal lineages in which identities of groups of neurons are specified (Jan and Jan, 1994). Mechanisms to regulate receptors for long-range repulsive and attractive cues are among the properties that each differentiated neuron acquires.

The mechanism by which attractive and repulsive cues act to shape neural architecture is most elegantly demonstrated in the midline of the *Drosophila* embryo. A combinatorial expression of Robo receptors respond to the diffusible ligand

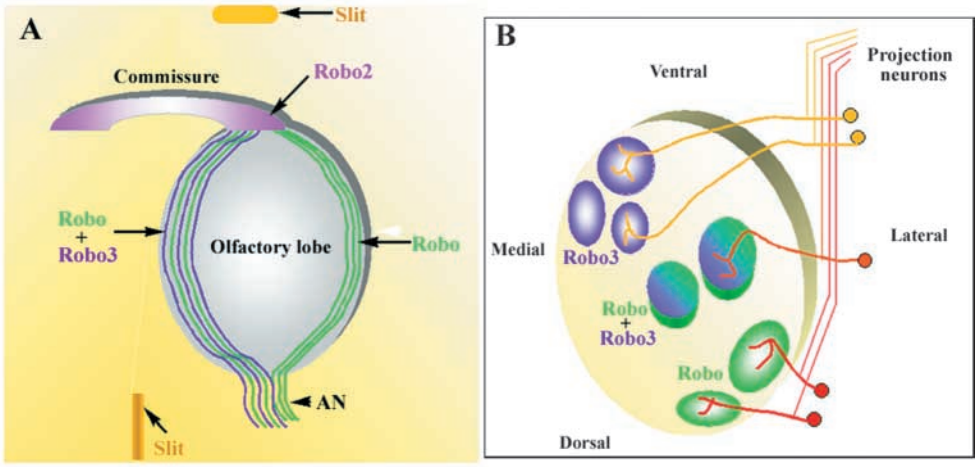

Fig. 6. Model for the role of Slit-dependent Robo signaling in glomerular patterning. (A) Sensory neurons enter the lobe via the antennal nerve (AN) and radiate over the olfactory lobe. Neurons expressing Robo (green) and Robo3 (purple) segregate from those expressing Robo alone and decussate onto the medial side. Robo2 (pink) expression is elevated after neurons have crossed in the commissure. Regions of Slit expression at the midline and in the brain are indicated by yellow bars. The yellow shading indicates the proposed Slit gradient. (B) Sensory neurons invade the lobe starting at ~25 APF. The positioning of terminals within the lobe is based on the Robo code (green, Robo; purple, Robo3) that they express and the differential response to Slit levels (yellow). The targeting of sensory neurons to specific positions allows short-range interactions with the projection neurons which are already present in the lobe. This leads to consolidation of the glomeruli, which become ensheathed by glial cell processes. The ventral, medial and lateral axis are indicated.

Slit to dictate positioning of axons within longitudinal tracts (Rajgopalan et al., 2000a; Rajgopalan et al., 2000b; Simpson et al., 2000a; Simpson et al., 2000b). At the midline, commissural neurons downregulate receptor expression by Comm-mediated protein degradation (Rosenzweig and Garrity, 2002). Similar principles guide the selection and shaping of axon fascicles in the retinotectal system of the zebrafish, as well as several major pathways in mammalian brains (Hutson and Chien, 2002; Plump et al., 2002; Bagri et al., 2002). The general principle of growth cone repulsion by Slit-mediated Robo signaling appears to be a conserved theme in circuit design (Richards, 2002).

Can a similar mechanism be exploited to determine the location of synapses in three-dimensional space? Ziatic et al. (Ziatic et al., 2003) have chosen projections from the chordotonal organs specified by Ato to demonstrate how Robo3 can specify location of sensory arbors in the central nervous system. The terminals act as substrate upon which synaptic interactions with second-order neurons are built leading to formation of connectivity. A similar process also appears to operate in giant fiber system of adult *Drosophila*, where Robo receptors have been shown to play key roles in synapse formation (Godenschwege et al., 2002). We envisage a comparable developmental strategy in the olfactory lobe of the *Drosophila* adult. The correct spatial and temporal regulation of Robo receptors and their response to Slit levels determines the positioning of neurons and branching of terminal arbors at specified positions within the lobe. This facilitates short-range interactions with appropriate projection neurons which are already present within the developing olfactory lobe (Jefferis et al., 2003).

Role of the secreted ligand Slit

Although the source and nature of the Slit gradient within the developing olfactory system remains obscure, we have demonstrated that an alteration in levels by ectopic expression leads to aberrant lobe patterning. Slit exerts growth cone repulsion at the *Drosophila* embryonic midline through its action on Robo receptors, as well as by silencing the attractive cues of Netrins by action on the DCC receptor (Stein and Tessier-Lavigne, 2001; Giger and Kolodkin, 2001). In the cortex of the mammalian brain, Slit is widely and dynamically expressed and exerts a major role on dendritic growth and branching (Zinn and Sun, 1999; Whitford et al., 2002). Studies on cortical cultures demonstrated that concentrations of Slit strongly affect dendritic length as well as number of branch-points per cell. Hence, the complex geometry of a Slit gradient during development and its ability to induce attraction, repulsion, as well as branching, could provide a means to sculpt axon pathways in three-dimensional space.

Multiple signaling systems instruct formation of a precise functional olfactory map

The stereotypic location of each glomerulus within the lobe, and the connectivity within and between glomeruli, are important aspects of information processing in these functional units (Rodrigues, 1988; Galazia and Menzel, 2000; Fiala et al., 2002; Ng et al., 2002; Wang et al., 2003). The relatively conserved pattern of olfactory glomeruli within different individuals suggests a robust developmental program for their formation.

The effects of Robo loss of function are incompletely penetrant and suggest that multiple signals must exist for targeting of neurons. We propose that the Robo receptors act in concert with DSCAM isoforms to guide sensory neurons to the ~50 unique positions within the three dimensional architecture of the lobe (Hummel et al., 2003). DSCAM and also Robo signaling could converge onto the Dock/Pak module, mutations in which also result in targeting defects (Ang et al., 2003; Fan et al., 2003). An accurate spatiotemporal estimation of receptors, ligands and signaling cascades across the developing olfactory lobe, together with mathematical modeling could provide valuable insights about the determination of glomerular patterns. Such knowledge is likely to be more generally applicable in the analysis of more complex brain structures including those of vertebrates.

We are grateful to Marina Voloshina and Niranjan Gaikwad for generating recombinant strains. We are indebted to Guy Tear, Erich Buchner, Gerd Technau, Leslie Vosshall, Andrew Jarman, Barry Dickson and Corey Goodman who providing us with many fly stocks and antibodies. We gratefully acknowledge K. VijayRaghavan, Satyajit Mayor and Michael Bate for their interest and valuable discussions; and K. VijayRaghavan and Mani Ramaswami for comments on the manuscript. This work was funded by grants from HFSP (RG0134), the Kanwal Rekhi Fellowship (to D.J. and A.S.) and core funding from TIFR.

References

Ang, L. H., Kim, J., Stepensky, V. and Hing, H. (2003). Dock and Pak regulate olfactory axon pathfinding in *Drosophila*. *Development* **130**, 1307-1316.

Bagri, A., Marin, O., Plump, A. S., Mak, J., Pleasure, S. J., Rubenstein, J. L. and Tessier-Lavigne, M. (2002). Slit proteins prevent midline crossing and determine the dorso-ventral position of the major axonal pathways in the mammalian forebrain. *Neuron* **33**, 233-248.

Bashaw, G. J., Kidd, T., Murray, D., Pawson, T. and Goodman, C. S. (2000). Repulsive axon guidance: abelson and enabled play opposing roles downstream of the roundabout receptor. *Cell* **101**, 703-715.

Bhalerao, S., Sen, A., Stocker, R. and Rodrigues, V. (2003). Olfactory neurons expressing identified receptor genes project to subsets of glomeruli within the antennal lobe of *Drosophila melanogaster*. *J. Neurobiol.* **54**, 577-592.

Buck, L. (2000). The molecular architecture of odor and pheromone sensing in mammals. *Cell* **100**, 611-618.

Cutforth, T., Moring, L., Mendelsohn, M., Nemes, A., Shah, N. M., Kim, M. M., Frisen, J. and Axel, R. (2003). Axonal Ephrin-As and odorant receptors: Coordinate determination of the olfactory sensory map. *Cell* **114**, 311-322.

Dickson, B. (2001). Rho GTPase in growth cone guidance. *Curr. Opin. Neurobiol.* **11**, 103-110.

Fan, X., Labrador, J. P., Hing, H. and Bashaw, G. J. (2003). Slit stimulation recruits Dock and Pak to the roundabout receptor and increases Rac activity to regulate axon repulsion at the CNS midline. *Neuron* **401**, 113-127.

Fiala, A., Spall, T., Diegelmann, S., Eisermann, B., Sachse, S., Devaud, J. M., Buchner, E. and Galizia, C. G. (2002). Genetically expressed cameleon in *Drosophila melanogaster* is used to visualize olfactory information in projection neurons. *Curr. Biol.* **12**, 1877-1884.

Fritz, J. L. and VanBerkum, M. F. A. (2002). Regulation of Rho family GTPases is required to prevent axons from crossing the midline. *Dev. Biol.* **252**, 46-58.

Galazia, C. G. and Menzel, R. (2000). Odour perception in honeybees: coding information in glomerular patterns. *Curr. Opin. Neurobiol.* **10**, 504-510.

Gao, Q., Yuan, B. and Chess, A. (2000). Convergent projections of *Drosophila* olfactory neurons to specific glomeruli in the antennal lobe. *Nat. Neurosci.* **3**, 780-785.

Giger, R. J. and Kolodkin, A. L. (2001). Silencing the Siren: guidance cue hierarchies at the CNS midline. *Cell* **105**, 1-4.

Godenschwege, T. A., Simpson, J. H., Shan, X., Bashaw, G. J., Goodman, C. S. and Murphey, R. K. (2002). Ectopic expression in the giant fiber system of *Drosophila* reveals distinct roles for roundabout (robo) Robo2 and Robo3 in dendritic guidance and synaptic connectivity. *J. Neurosci.* **22**, 3117-3129.

Grunvald, I. C. and Klein, R. (2002). Axon guidance: receptor complexes and signaling mechanisms. *Curr. Opin. Neurobiol.* **12**, 250-259.

Hassan, B. A., Bermingham, N. A., He, Y., Sun, Y., Jan, Y. N., Zoghbi, H. Y. and Bellen, H. (2000). Atonal regulates neurite arborization but does not act as a proneural gene in the *Drosophila* brain. *Neuron* **25**, 549-561.

Hummel, T., Vasconcelos, M. L., Clemens, J. C., Fishilevich, Y., Vosshall, L. B. and Zipursky, S. L. (2003). Axonal targeting of olfactory receptor neurons in Drosophila is controlled by Dscam. *Neuron* **37**, 221-231.

Hutson, L. D. and Chien, C. B. (2002). Pathfinding and error correction by retinal axons: the role of astray/robo2. *Neuron* **33**, 205-217.

Jan, Y. N. and Jan, L. Y. (1994). Genetic control of cell fate specification in the peripheral nervous system. *Annu. Rev. Genet.* **28**, 373-393.

Jefferis, G. S. X. E., Marin, E. C., Stocker, R. F. and Luo. L. (2001). Target neuron prespecification in the olfactory map of *Drosophila*. *Nature* **414**, 204-208.

Jefferis, G. S. X. E., Marin, E., Watts, R. J. and Luo, L. (2002). Development of neuronal connectivity in Drosophila antennal lobes and mushroom bodies. *Curr. Opin. Neurobiol*. **12**, 80-86.

Jefferis, G. S. X. E., Vyas, R. M., Berdnik, D., Ramaekers, A., Stocker, R. F., Tanaka, N. K., Ito, K. and Luo, L. (2003). Developmental origin of wiring specificity in the olfactory system of *Drosophila*. *Development* **131**, 117-130.

Jhaveri, D. and Rodrigues, V. (2002). Sensory neurons of the Atonal lineage pioneer the formation of glomeruli within the adult *Drosophila* olfactory lobe. *Development* **129**, 1251-1260.

Jhaveri, D., Sen, A. and Rodrigues, V. (2000). Mechanisms underlying olfactory neuronal connectivity in *Drosophila* – the Atonal lineage organizes the periphery while sensory neurons and glia pattern the olfactory lobe. *Dev. Biol.* **226**, 73-87.

Kidd, T., Bland, K. S. and Goodman, C. S. (1999). Slit is the midline repellent for the Robo receptor in Drosophila. *Cell* **96**, 785-794.

Knoll, B., Schmidt, H., Andrews, W., Guthrie, S., Pini, A., Sundaresan, V. and Drescher, U. (2003). On the topographic targeting of basal vomeronasal axons through Slit-mediated chemorepulsion. *Development* **130**, 5073-5082.

Komiyama, T., Johnston, W. A., Luo, L. and Jefferies, G. S. X. E. (2003). From lineage to wiring specificity: POU domain transcription factors control precise connections of Drosophila olfactory projection neurons. *Cell* **112**, 157-167.

Laissue, P. P., Reiter, C., Hiesinger, P. R., Halter, S., Fischbach, K. F. and Stocker, R. F. (1999). Three-dimensional reconstruction of the antennal lobe in *Drosophila melanogaster*. *J. Comp. Neurol.* **22**, 543-552.

Lebetsky, T., Chang, T., Hartenstein, V. and Banerjee, U. (2000). Specification of Drosophila hematopoietic lineage by conserved transcription factors. *Science* **288**, 146-149.

Lee, T. and Luo, L. (1999). Mosaic analysis with a repressible cell marker for studies of gene function in neuronal morphogenesis. *Neuron* **22**, 451-461.

Marin, E. C., Jefferis, G. S. X. E., Komiyama. T., Zhu, H. and Luo, L. (2002). Representation of the glomerular olfactory map in the Drosophila brain. *Cell* **109**, 243-255.

Newsome, T. P., Asling, B. and Dickson, B. J. (2000). Analysis of Drosophila photoreceptor axon guidance in eye-specific mosaics. *Development* **127**, 851-860.

Ng, M., Roorda, R. D., Lima, S. Q., Zemelman, B. V., Morcillo, P. and Meisenbock, G. (2002). Transmission of olfactory information between three populations of neurons in the antennal lobe of the fly. *Neuron* **36**, 463-474.

Plump, A. S., Erskine, L., Sabatier, C., Brose, K., Epstein, C. J., Goodman, C. S., Mason, C. A. and Tessier-Lavigne, M. (2002). Slit1 and Slit2 cooperate to prevent premature midline crossing of retinal axons in the mouse visual system. *Neuron* **33**, 219-232.

Rajagopalan, S., Nicolas, E., Vivancos, V., Berger, J. and Dickson, B. J. (2000a). Crossing the midline: Roles and regulation of Robo receptors. *Neuron* **26**, 767-777.

Rajagopalan, S., Vivancos, V., Nicolas, E. and Dickson, B. J. (2000b). Selecting a longitudinal pathway: Robo receptors specify the lateral position of axons in the Drosophila CNS. *Cell* **103**, 1033-1045.

Richards, L. J. (2002). Surrounded by Slit-how forebrain commissural axons can be led astray. *Neuron* **33**, 153-155.

Rodrigues, V. (1988). Spatial coding of olfactory information in the antennal lobe of *Drosophila melanogaster*. *Brain Res.* **453**, 299-307.

Rosenzweig, M. and Garrity, P. (2002). Axon targeting meets protein trafficking: Comm takes Robo to the cleaners. *Dev. Cell* **3**, 301-302.

Rothberg, J. M., Jacobs, J. R., Goodman, C. S. and Artavanis-Tsaklonas, S. (1990). *Slit*: an extracellular protein necessary for development of midline glia and commissural axons pathways contains both EGF and LRR domains. *Genes Dev.* **4**, 2169-2187.

Schmucker, D., Clemens, J. C., Shu, H., Worby, C. A., Xiao, J., Muda, M., Dixon, J. E. and Zipursky, S. L. (2000). *Drosophila* Dscam is an axon guidance receptor exhibiting extraordinary molecular diversity. *Cell* **101**, 671-684.

Shymala, B. V. and Chopra, A. (1999). *Drosophila melanogaster* chemosensory and muscle development: identification and properties of a novel allele of *scalloped* and a new locus SG18.1, in a Gal4 enhancer trap screen. *J. Genet.* **78**, 87-97.

Simpson, J. H., Simpson, J. H., Bland, K. S., Fetter, R. D. and Goodman, C. S. (2000a). Short-range and long-range guidance by Slit and its Robo receptors: a combinatorial code of Robo receptors control lateral position. *Cell* **103**, 1019-1032.

Simpson, J. H., Kidd, T., Bland, K. S. and Goodman, C. S. (2000b). Short-range and long-range guidance by Slit and its Robo receptors: Robo and Robo2 play distinct roles in midline guidance. *Neuron* **28**, 753-766.

Stein, E. and Tessier-Lavigne, M. (2001). Hierarchical organization of guidance receptors: Silencing of netrin attraction by slit through a Robo/DCC receptor complex. *Science* **291**, 1928-1938.

Stocker, R. F., Lienhard, M. C., Borst, A. and Fischbach, K. F. (1990). Neuronal architecture of the antennal lobe in *Drosophila melanogaster*. *Cell Tissue Res.* **262**, 9-34.

Stocker, R. F. (1994). The organization of the chemosensory system in *Drosophila melanogaster*: a review. *Cell Tissue Res.* **275**, 3-26.

Vosshall, L. B., Wong, A. M. and Axel, R. (2000). An olfactory sensory map in the fly brain. *Cell* **102**, 147-159.

Wang, F., Nemes, A., Mendelsohn, M. and Axel, R. (1998). Odorant receptors govern the formation of a precise topographic map. *Cell* **93**, 47-60.

Wang, J. W., Wong, A. M., Flores, J., Vosshall, L. B. and Axel, R. (2003). Two-photon calcium imaging reveals an odor-evoked map of activity in the fly brain. *Cell* **112**, 271–282.

Whitford, K. I., Marillat, V., Stein, E., Goodman, C. S., Tessier-Lavigne, M., Chedotal, A. and Ghosh, A. (2002). Regulation of cortical dendrite development by Slit-Robo interactions. *Neuron* **33**, 47-61.

Wong, A. M., Wang, J. W. and Axel, R. (2002). Spatial representation of the glomerular map in the Drosophila protocerebrum. *Cell* **109**, 229-241.

Ziatic, M., Landraf, M. and Bate, M. (2003). Genetic specification of axonal arbors: *atonal* regulates *robo3* to position terminal branches in the *Drosophila* nervous system. *Neuron* **37**, 41-51.

Zinn, K. and Sun, Q. (1999). Slit branches out: a secreted protein mediates both attractive and repulsive axon guidance. *Cell* **97**, 1-4.